# A COMPARATIVE STUDY OF THE VARIABLE SCREENING AND HARTREE–FOCK MODELS AS MEANS FOR THE CONSTRUCTION OF TWO-CENTER CORRELATION DIAGRAMS

Jan LORINCIK[a], Rudolf POLAK[a], Zdenek SROUBEK[b] and Ivana PAIDAROVA[a]

[a] *J. Heyrovsky Institute of Physical Chemistry, Academy of Sciences of the Czech Republic, 182 23 Prague 8, The Czech Republic*

[b] *The Institute of Radioelectronics, Academy of Sciences of the Czech Republic, 182 51 Prague 8, The Czech Republic*

Received August 22, 1994
Accepted December 11, 1994

The aim of this work is to test the Variable Screening Model (VSM) [Wille U., Hippler R.: Phys. Rep. *132*, 129 (1986)] as a method for computing correlation diagrams of neutral and ionized diatomic quasimolecules by comparing the results with corresponding Hartree–Fock calculations, and to elucidate the specific features of both aforementioned approaches in applications to given purpose. These calculations serve as the first step in the interpretation of inner-shell vacancy production in low-velocity ion–atom collisions inside bombarded solids.

The motivation for this work came from the need to interpret ion–solid interactions, playing role in some physical phenomena, like in ion-induced electron emission[1] and in SIMS (Secondary Ion Mass Spectrometry) experiments. Understanding of the mechanisms of secondary ion creation in SIMS is of great theoretical and practical importance.

Secondary ion formation can be also caused in collision cascades by energetic encounters between the primary ion and target atom (PT), as well as between target atoms (TT) themselves. This effect has been observed in connection with positive ion emission from the light elements Al, Mg and Si under usual sputtering conditions[2]. The secondary ion yields from these elements increase significantly with the primary ion energy, and unusually high multiply-charged positive secondary ion yields are observed at noble gas bombardment. Experimental findings[2] suggest that the major reason for the ionization of multiply-charged sputtered atoms is the presence of core holes created in energetic collisions. The most widely accepted mechanism for the production of such inner-shell excitations is the electron-promotion model developed originally by Fano and Lichten[3] for atomic collisions. Recently, an extension of this approach to processes in solids has been published[4].

The first step in describing these mechanisms within the one-electron approximation represents the calculation of adiabatic MO correlation diagrams and wave functions for

quasimolecules. A conceptually simple picture, allowing a straightforward computation of correlation diagrams and associated wave functions for any given combination of collision partners, gives the variable screening model developed by Eichler and Wille[5–8] by using the two-center Thomas–Fermi potential. This model is based on the idea that the mutual screening of the atoms making up the quasimolecule may be well approximated by spherical functions in which the screening of nuclear charges varies with the internuclear distance. Accordingly, an effective single-electron potential represented as a sum of two spherical potentials, each centered on one of the colliding nuclei, is proposed. These potentials are obtained by smoothly interpolating the screening parameters of suitable atomic potentials (Thomas–Fermi–Dirac (TFD) or phenomenological potentials) between the united-atom and the separated-atom limits.

In this paper correlation diagrams for several diatomic systems calculated by the VSM and standard Hartree–Fock methods are compared in order to provide an illustrative background for discussing the properties of the adiabatic MO correlation diagrams obtained by different types of approaches.

## THEORETICAL

### *Calculation of One-Electron Correlation Diagrams and Wave Functions*

*Variable screening model.* Within VSM, the model one-electron Hamiltonian[5,7] (in atomic units) for a diatomic quasimolecule may be written as

$$\mathbf{H}(r_1,r_2,R) = -1/2\nabla^2 + V^{\mathrm{eff}}(r_1,r_2,R) \ , \qquad (1)$$

where $r_1,r_2$ are the distances of the electron from the two nuclei, and $R$ is the internuclear separation. The effective potential is constructed from single-electron potentials $V(r) = -Z\,\Phi(r,\alpha)/r$, where $Z$ is the charge number and the parameter in the screening function $\Phi(r,\alpha)$ denotes collectively a set of parameters assigned to the united atom ($\alpha^{\mathrm{ua}}$) and separated atoms ($\alpha_i^{\mathrm{sa}}$) screening functions. For expressing the effective screening parameter $\alpha_i^{\mathrm{eff}}$ we adopted the interpolation scheme[5,7]

$$\alpha_i^{\mathrm{eff}} = \frac{\alpha_i^{\mathrm{sa}}\,\lambda^2 + \alpha^{\mathrm{ua}}\,\rho_i^2}{\lambda^2 + \rho_i^2} \ , \qquad (2)$$

where $\rho_i = 2r_i/R$ ($i$ = 1, 2) and the parameter $\lambda^2$ acquires values[7] between 2 and 4. The final form for the approximated molecular single-electron potential is then[7]

$$V^{\mathrm{eff}}(r_1,r_2,R) = -\frac{Z_1}{r_1}\,\Phi(r_1,\alpha_1^{\mathrm{eff}}) - \frac{Z_2}{r_2}\,\Phi(r_2,\alpha_2^{\mathrm{eff}}) \ , \qquad (3)$$

which is most conveniently expressed in terms of prolate spheroidal coordinates $\xi = \frac{(r_1 + r_2)}{R}$ , $\eta = \frac{(r_1 - r_2)}{R}$ , and the azimuthal angle φ around the internuclear axis. The screening functions were chosen as Thomas–Fermi–Dirac functions in the form of Latter's analytical expression[9] or the independent-particle-model (IPM) potential of Green, Sellin and Zachor[10] (GSZ). In the latter approximation, the atomic and ionic screening functions are written[5,11]

$$\Phi(r;K,d) = (1 - p)\,\Omega(r) + p \qquad (4a)$$

with

$$\Omega(r) = [Kd\,(\mathrm{e}^{r/d} - 1) + 1]^{-1} \qquad (4b)$$

and

$$p = (k + 1)/Z \ , \qquad (4c)$$

where $k$ is the degree of ionization ($k = 0$ for neutrals). For given $Z$ and $k$, the parameter values of $K$ and $d$ can be found in ref.[11].

The resulting two-center one-electron Schrödinger equation

$$[\mathbf{H}(\xi,\eta,\varphi,R) - E(R)]\,\Psi(\xi,\eta,\varphi) = 0 \qquad (5)$$

may conveniently be solved[7] by expanding the wave function Ψ in terms of Hylleraas-type functions[12]

$$\Psi_{nl}^{m}(\xi,\eta,\varphi) = (\xi^2 - 1)^{m/2}\,\mathrm{e}^{-x/2}\,\mathrm{L}_n^m(x)\,\mathrm{P}_l^m(\eta)\,\mathrm{e}^{\mathrm{i}m\varphi} \ , \qquad (6)$$

where $x = (1/a)(\xi - 1)$ ($a$ being a parameter affecting the convergence properties of the solution), $L_n^m(x)$ and $P_l^m(\eta)$ are the generalized Laguerre polynomials and the associated Legendre functions, respectively.

Similarly as in ref.[7] , the matrix elements of the kinetic energy operator $\mathbf{T} = -1/2\nabla^2$ as well as the overlap matrix elements were evaluated analytically, the matrix elements involving potential terms were computed numerically. The calculation of integrals was performed in prolate spheroidal coordinates by using combined Gauss–Laguerre or Gauss–Legendre formulae.

An alternative way of solving Eq. (*5*) consists in expanding the wave function $\Psi$ in terms of a limited set of atomic one-electron wave functions (e.g. Slater-type orbitals). Such an approach within VSM has been described earlier[13] and will be also used in some of our calculations. To distinguish between the two types of VSM calculations, we will use the labelling VSM I and VSM II for the Hylleraas- and atomic wave-function-type solutions, respectively.

*Hartree–Fock method*. The SCF calculations of RHF or ROHF type were performed by using the GAMESS system[14]. Universally, as the atomic orbital basis sets the "valence triple zeta" bases of McLean and Chandler were employed[15], with the exception of the Ge-system for which the Binning–Curtiss "double zeta" basis set[16] was used.

## RESULTS AND DISCUSSION

### *The Ne–Ne System*

Ne–Ne is an appropriate system for testing our VSM computer codes and the adequateness of AO basis set selections for SCF calculations, because there exist previous constructions of correlation diagrams not only by means of VSM using both TFD (ref.[6]) and GSZ (ref.[7]) potentials, but also by an *ab initio* Hartree–Fock MO calculation[17]. Comparison of Fig. 1 with the corresponding figure of ref.[6] reveals that the graphical representation of our VSM I calculation (TFD potential) can be considered identical to the correlation diagram of the Ne–Ne system presented in ref.[6]. Although in the diagram of Larkins[17] some higher one-electron states ( which are present in our diagram) are missing, it may be stated that the *R*-dependences of orbital energies coming from both SCF calculations, including the position of the avoided crossing between the $2\sigma_g$ and $3\sigma_g$ states, compare favourably.

The GSZ atomic potential is superior to the TFD one in that it can be easily parameterized so as to achieve an accurate reproduction of given atomic electronic structure. In addition, it facilitates the modification of atomic potentials to encompass the description of ionized species. Therefore, in further VSM applications the analytical independent-particle potential of Green, Sellin and Zachor[10] will be applied in the effective potential Eq. (*3*).

In Fig. 2 the VSM correlation diagram is displayed which was calculated by using the phenomenological parameter selection suggested by Garvey et al.[11]. For comparison, in this figure there are also included results of our restricted Hartree–Fock calculation. Whereas the agreement of the two types of calculation is satisfactory in the interval of the internuclear distances 0.5 – 2 a.u., for larger internuclear distances (about above 3 a.u.) the orbital energies computed by VSM are higher and monotonically increasing with increasing the internuclear distance. Moreover, the couples of curves corresponding to associated g and u states do not tend to a common separated-atom limit as it should be for a homonuclear system. These special effects, which might be reduced to a physically unimportant proportion by a suitably chosen basis set extension, are inherent to a model case of one electron moving in the field of two screened Coulomb centers, the solution of which is looked for in the form of expansion (*6*). Some implications connected with the one-electron screened-unscreened two-center problem have been discussed in ref.[7].

In the next step of our study we tried to fit RHF data by adjusting the driving parameters in VSM I calculations. We have found that choosing $a = 0.82/R$ (at $n_{max} = 6$

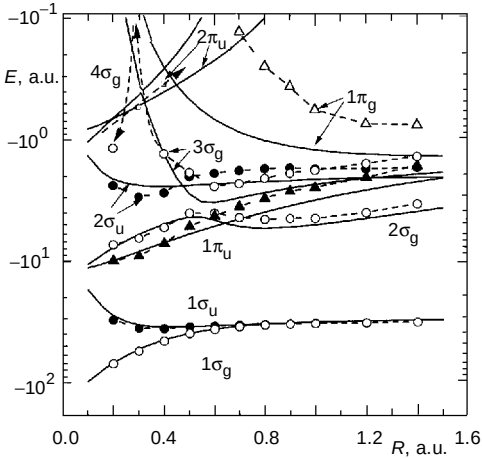


FIG. 1
Adiabatic MO correlation diagram for Ne–Ne calculated within the VSM using TFD potential (full lines), and the SCF model (dashed lines). Symbols are used to represent SCF calculations in Figs 1 through 7

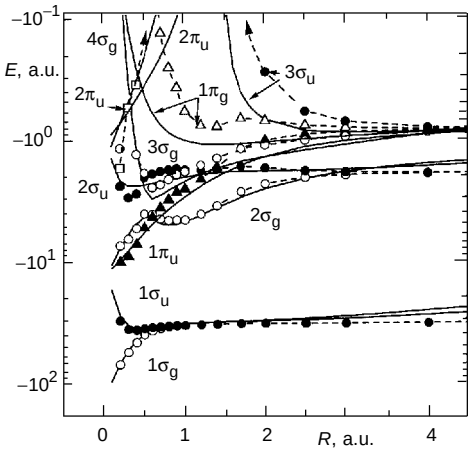


FIG. 2
Adiabatic MO correlation diagrams for Ne–Ne calculated by VSM using the GSZ potential (full curves). The parameter values utilized in the calculation are $\lambda^2 = 3$, $a = 0.2/R$, $n_{max} = 6$, $l_{max} = 7$. Potential parameters ($K$, $d$) were calculated from those taken from ref.[11]. The calculation has been restricted to $\sigma(m = 0)$ and $\pi(m = 1)$ states. The SCF calculations are represented by dashed lines

and $l_{max} = 7$) one obtains VSM $3\sigma_g$ and $2\sigma_u$ states as close as possible to the SCF ones. However, the cost paid for this local coincidence is the deterioration of the other parts of the correlation diagram lying in the regions of $-10^2$ – $-10^1$ a.u. and around zero of electronic energies. Further parameter variations led us to the conclusion, that the best results for the given basis set ($n_{max} = 6$, $l_{max} = 7$) can be achieved for $a$ being close to $0.2/R$; generally, the decrease of $a$ leads to an orbital energy shift towards higher values.

In Fig. 3 we demonstrate the influence of the parameters $n_{max}$, $l_{max}$ ($(n_{max} + 1)$ $(l_{max} + 1)$ is the number of basis functions for $m = 0$), i.e. the basis set size, on the correlation diagrams. The increase of the basis set size has clearly salutary effects to all shortcomings of the VSM solution appearing at larger internuclear separations discussed above: orbital-level shift to higher energies and violation of the degeneracy of states at separated-atom limit. Also, the dissociation energy limits become closer to the SCF values.

Finally it was observed that variation of the parameter $\lambda^2$ had smaller effect on the calculated energies than the other parameters.

*The $Ne^{2+}$–Ne System*

The interest in experimental studies on interaction of highly charged ions with solid surfaces is steadily increasing[18]. Therefore, it is opportune to develop models for corre-

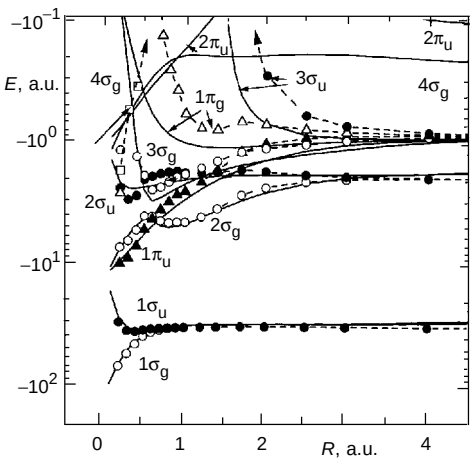


FIG. 3
Adiabatic MO correlation diagrams for Ne–Ne. Expansion parameters $n_{max} = 8$, $l_{max} = 9$, for remaining parameter values and further specifications see captions to Figs 1 and 2

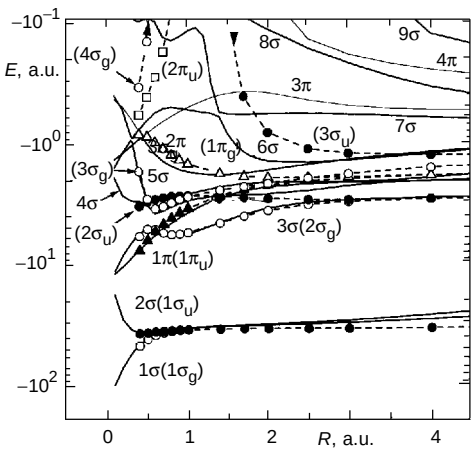


FIG. 4
Adiabatic MO correlation diagrams for the charge-imbalanced system $Ne^{2+}$–Ne (full curves) as calculated by VSM I (for the parameter definition see Fig. 2), and for the $(Ne–Ne)^{2+}$ system (symbols + dashed lines) calculated by the SCF method

lation diagram construction of charged quasimolecules. Because of the projectile ionization, the incoming channel of an ion-atom encounter represents a charge-imbalanced system, which corresponds to an excited state of the adiabatically relaxed quasimolecule. Figure 4 presents our VSM calculation of the correlation diagram for the $Ne^{2+}$–Ne system. We compare it with the RHF orbital energies for the quasimolecular ground state of $(Ne–Ne)^{2+}$ treated as a homonuclear system, i.e. with the inversion-symmetry-adapted solution. The obvious differences lie in the existence of avoided crossings and the marked splitting of some VSM valence states in the separated-atom limit indicating the asymmetry of the $Ne^{2+}$–Ne system[7], in contrast to the (homonuclear) symmetry-adapted SCF solution. However, the agreement of the orbital energy values for the charged Ne–Ne quasimolecule, as they are provided by both methods, is surprisingly good which can be explained by charge equilibration for small distances ($R < 2$ a.u.).

*Fluorides*

A stimulating impulse for the calculation of correlation diagrams for fluor containing diatomics came from the need to interpret recent measurements of $F^+$ ion emission and electron emission from fluorides (LiF, $LaF_3$, $CeF_3$) under noble gas atom or ion (Ar, Xe and He ) bombardment[13,19]. The characteristic feature of these experiments is a high yield of secondary $F^+$ ions, despite the high ionization energy and strong dependence of the yield on the type and the state of projectile. One of the interpretations involves a double hole creation in $F^-$ by an electron promotion process during $F^-$-projectile collisions in which two electrons from 2*p* orbitals of $F^-$ are transferred and dissipated in the conduction band of the fluoride (LiF, ref.[13]). As a model system for the $F^-$-projectile inside fluoride can serve $F^0$, as $F^-$ is stabilized inside fluoride by the Madelung energy which shifts the levels of $F^-$ so that they are close to the energy levels of neutral fluorine outside the solid.

In Fig. 5 we present adiabatic correlation diagrams for the F–He system calculated by VSM I, VSM II ($\sigma$-orbitals only[13]) and the SCF method. The separated-atom F 2*p* orbital evolves into the $4\sigma$ and $1\pi$ quasimolecular F–He orbitals in the course of atom–atom approach. The promotion of the $4\sigma$ orbital begins at $\approx$2.5 a.u. and crosses the bottom of the conduction band (which is around zero energy) at the distance of about 1.2 a.u. Also shown in the Fig. 5 are the minimum kinetic energies (in eV, calculated from the potential function of Molière[20]) in head-on collisions needed to reach the interatomic distances marked by arrows.

In Fig. 6 we show the same types of diagrams as in Fig. 5 for the Ar–F system. Here the F 2*p* orbital evolves into the $7\sigma$ and $2\pi$ quasimolecular F–Ar orbitals. The promotion of the $7\sigma$ orbital starts at $\approx$1 a.u. and crosses the bottom of the conduction band at the distance of about 0.5 a.u. Similarly as in the previous figure, kinetic energies (in eV) needed to reach distinct interatomic distances are indicated.

The agreement in orbital energy values for all three methods is reasonable with the exception of the VSM I method for larger separations and high orbital energies (above $\approx -6.0 \cdot 10^{-1}$ hartree, Ar $3p \rightarrow 8\sigma$ orbital). This discrepancy can be partially removed by basis set extension (see discussion to the Ne–Ne system).

On grounds of comparing Figs 5 and 6 it might be conjectured that the ionization of fluorine by the electron promotion mechanism requires by one or two orders of magnitude less kinetic energy for He bombardment than for Ar bombardment. This correlates well with the measured $F^+$ yield from the bombarded LiF (ref.[13]).

*The Ge–Ge System*

Also the theoretical work on the Ge–Ge system was undertaken because of recently performed measurements of energy distribution of electrons emitted from Ge under Ar bombardment[21]. Elucidation of the high yield of secondary electrons emitted from Ge in terms of inner-shell excitation mechanisms requires a correlation diagram which can provide answers to questions like: Which orbital is promoted? How efficiently? How much kinetic energy is required for the efficient promotion? What is the threshold energy?

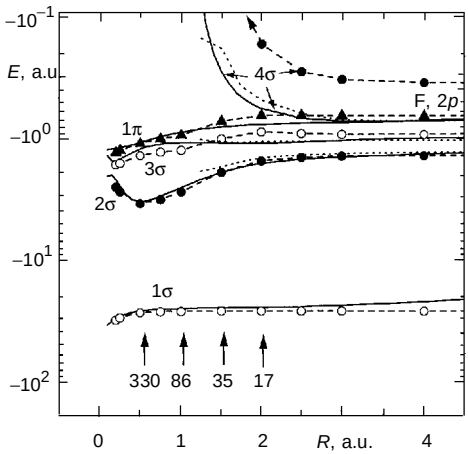


FIG. 5
Adiabatic MO correlation diagrams for He–F as calculated by VSM I (full curves), VSM II (dotted curves) and ROHF (symbols + dashed lines). For the expansion parameters see Fig. 2. The distances of closest approach in head-on collisions for different kinetic energies (eV, in the center of mass system) are shown by arrows

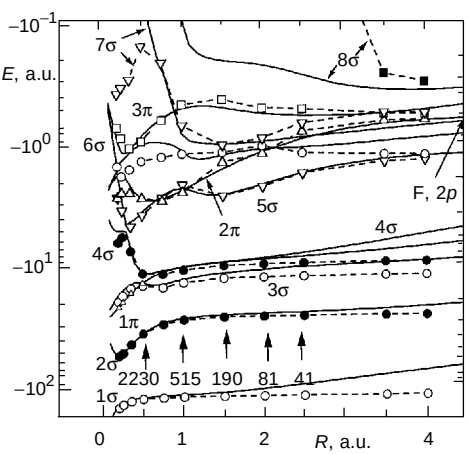


FIG. 6
Adiabatic MO correlation diagrams for Ar–F. The details are the same as in Fig. 5

In Fig. 7 we present adiabatic correlation diagrams for Ge–Ge calculated by VSM I and by the RHF method. In order to effectively visualize this 64-electron system, the graphical representation of orbital correlations is separated into two parts; in Fig.7*a* σ-orbital energies, and in Fig. 7*b* π and δ orbital energies are disclosed.

Similarly as in previous cases, the optimum agreement between the two methods is found at medium separations (0.7 – 2.0 a.u), and the VSM I results for larger internuclear distances can be brought closer to the SCF ones by a basis set extension. At very short separations both methods cease to be reliable; evidently for $R < 0.2$ a.u. VSM would give better results by using the united-atom Thomas–Fermi potential.

Figure 8 serves the purpose to show the small oscillations on some of SCF energy curves (e.g. states $4\pi_u$, $7\sigma_g$, $3\pi_g$, $1\delta_u$ at separations between 1.2 and 1.5 a.u.). These irregularities are a consequence of changes in the SCF electronic potential which occur whenever an occupied MO at the Fermi surface of the molecular Hartree–Fock ground state crosses an unoccupied MO.

In Figs 7 and 8 we can identify the following promoted levels: $6\sigma_u$ (1.2 – 1.7 a.u.) and $3\pi_g$ (0.8 – 1.2 a.u.). One notices also that promotion is accompanied by a robust interplay of several adiabatic levels resulting in avoided crossings of energy levels. Arrows in Fig. 7 indicate minimum kinetic energies required in head-on collision to

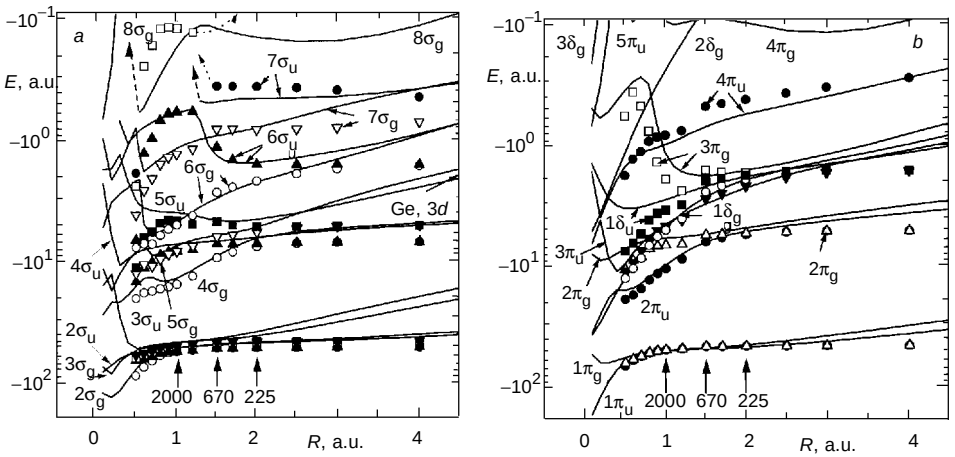


FIG. 7

Adiabatic MO correlation diagrams for Ge–Ge as calculated by VSM I (full curves) and the RHF method. Open and solid symbols are used to represent symmetric (g) and unsymmetric (u) states, respectively. The parameter values used in the calculations are $\lambda^2 = 3$, $a = 0.2/R$, $n_{max} = 8$, $l_{max} = 9$; potential parameters ($K$, $d$) were calculated from those taken from ref.[11]. The distances of closest approach in head-on collisions for different kinetic energies (eV, in the center of mass system) are shown by arrows. MO plotted: *a* σ orbitals ($m = 0$), *b* π and δ orbitals ($m = 1$ and $m = 2$)

reach given interatomic separations. From these figures it can be observed that the promotion of the $6\sigma_u$ level (i.e. Ge 3*d* orbital) could play the key role in electronic excitation of germanium atoms at their energetic collisions.

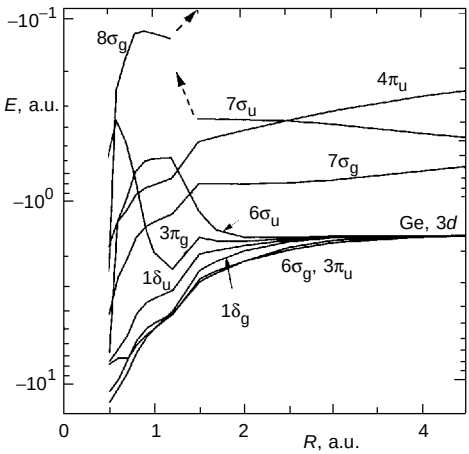


FIG. 8
Adiabatic MO correlation diagram for selected states of Ge–Ge as calculated by the RHF method. The data correspond to those which are represented separately in Figs 7*a* and 7*b*

## CONCLUSIONS

Besides giving qualitative explanation by means of particular electron promotion mechanisms to some atomic ion and electron emission experiments (fluorides, Ge under noble gas bombardment), this paper brings further evidence on the capacity and characteristic features of the variable screening model[5,7] as a method for constructing diatomic one-electron-state correlation diagrams. The study of the basic properties of the VSM method is done by comparing its performance with standard molecular Hartree–Fock calculations.

It was pleasant to note that both methods yield correlation diagrams which resemble each other to a great extent, with the largest agreement occurring at medium interatomic separations, ranging approximately from 0.5 to 3 a.u. At very short *R* values, where the Hartree–Fock method suffers sometimes from convergence difficulties, the VSM method might produce a reliable solution by using an appropriate united atom convergent potential. Without doubt VSM is superior to the standard SCF approach in treating encounters of charge-imbalanced systems[6] (e.g. $Ne^{2+}$ + Ne) in a physically correct way. A further positive feature of VSM is that it is able to describe consistently systems with incompletely filled electron shells. The insufficiencies of the VSM solution, associated with the orbital level shift to higher energies and the violation of degeneracy of states at separated-atom limit, might be partly overcome by basis extension.

One can therefore conclude that the variable screening model represents, with respect to its computational feasibility, an interesting alternative to the theoretical treatment of quasimolecular excitation mechanisms, particularly applicable to special problems, like inner-shell vacancy production in low-velocity ion-atom collisions, or in diatomics with a large number of electrons.

**REFERENCES**


1. Baragiola R. A., Alonso E. V., Ferron J., Oliva-Florio A.: Surf. Sci. *90*, 240 (1979).
2. Yu M. L. in: *Sputtering by Particle Bombardment* (R. Behrish and K. Wittmaack, Eds), Vol III. Springer, Berlin 1993.
3. Fano U., Lichten W.: Phys. Rev. Lett. *14*, 627 (1965).
4. Sroubek Z., Falcone G. in: *Ionization of Solids by Heavy Particles* (R. A. Baragiola, Ed.). Plenum Press, New York 1993.
5. Wille U., Hippler R.: Phys. Rep. *132*, 129 (1986).
6. Eichler J., Wille U.: Phys. Rev. Lett. *33*, 56 (1974).
7. Eichler J., Wille U.: Phys. Rev., A *11*, 1973 (1975).
8. Kaufmann P., Wille U.: Z. Phys., A *279*, 259 (1976).
9. Latter R.: Phys. Rev. *99*, 510 (1955).
10. Green A. E. S., Sellin D. L., Zachor A. S.: Phys. Rev. *184*, 1 (1969).
11. Garvey R. H., Jackman C. H., Green A. E. S.: Phys. Rev. A *12*, 1144 (1975).
12. Hylleraas E.: Z. Phys. *71*, 739 (1931).
13. Sroubek Z., Oechsner H.: Surf. Sci. *311*, 263 (1994).
14. Dupuis M., Spangler D., Wendoloski J. J.: *NRCC Software Catalog*, Vol.1. Original program QG01 (GAMESS), 1980. Version by Schmidt M. W., Baedridge K. K., Boatz J. A., Jensen J. H., Koseki S., Gordon M. S., Nguyen K. A., Windus T. L., Elbert S. T.: QCPE Bulletin *10*, 52 (1990).
15. McLean A. D., Chandler G. S.: J. Chem. Phys. *72*, 5639 (1980).
16. Binning, R. C., jr., Curtiss L. A.: J. Comput. Chem. *11*, 1206 (1990).
17. Larkins F. P.: J. Phys., B *5*, 571 (1972).
18. Morgenstern P., Das J.: Europhys. News *25*, 1 (1994).
19. Lorincik J., Sroubek Z., Bastl Z.: Rad. Eff. Def. Sol. *128*, 127 (1994).
20. Moliere G.: Z. Naturforsch., A *2*, 133 (1947).
21. Fine J.: Unpublished results.